energy&fuels

Article

Performance Evaluation of Two 25 kW Residential Wood Pellet Boiler Heating Systems

Kui Wang,[†,‡] Mauro Masiol,[†] Devraj Thimmaiah,[†] Yuanyuan Zhang,[†] and Philip K. Hopke[*,†,‡]

[†]Center for Air Resources Engineering and Science and [‡]Department of Chemical and Biomolecular Engineering, Clarkson University, Potsdam, New York 13699, United States

S *Supporting Information*

ABSTRACT: A significant increase in the use of wood pellets for residential space heating has occurred over the past decade. The performance of two modern residential wood pellet boilers [designated Parishville boiler (PB) and West Potsdam boiler (WPB)] were evaluated, including boiler thermal efficiency, thermal energy storage (TES) tank discharge efficiency, and system efficiency. A correlation applicable to both systems between the boiler thermal efficiency (η_{th}, %) and the boiler output load (χ, %) was found in the form of $\eta_{th} = 52.69 \ln \chi - 137.7$, with $r^2 = 0.79$ (for $25 < \chi < 75$). This equation provides an easy, accurate estimation of the boiler thermal efficiency in field operations. The boiler thermal efficiency decreased with time, and this decline was determined using a Mann−Kendall trend analysis with Sen's slope. This decrease was primarily the result of fouling in the heat exchanger, and thus, this analysis identifies the need for manual cleaning of the heat exchanger tubes to restore maximal system performance. The evaluation of the TES tank performance found that the TES tank discharge efficiency was correlated with a dimensionless function of tank inlet Reynolds number (Re_d) and temperature differences in the tank and inlet and outlet pipes. Overall system efficiency showed a seasonal average of 62.8, 62.0, and 75.8% for three heating seasons of the PB system. These results provide a comprehensive performance evaluation of these wood pellet boiler heating systems in the field over an extended period of operation.

1. INTRODUCTION

Because of the increasing interest in the use of renewable energy, biomass has been increasingly used over the past decade. According to the International Energy Agency (IEA), bioenergy provides 10% of the world primary energy supply currently[1] and biofuels can provide up to 27% of the world transportation fuel by 2050.[2] Generally, biomass refers to any material that is derived directly or indirectly from plants.[3] Biomass, especially wood and wood pellets, is becoming more widely used as an alternative energy source for domestic space heating as a result of its relatively high energy density and uniform quality compared to cordwood or chips.[4] In the European Union, wood pellet use is growing rapidly as a result of government policies to meet renewable energy targets.[3−5]

Wood pellets offer both economic and climate benefits. Wood can be harvested sustainably, provide a substantial local energy supply, and offer extra employment to collect and process the wood. Chau et al.[6] provided a detailed techno-economic evaluation of a small-scale wood pellet heating system. Wood pellet boiler technology has also improved over the past few decades, particularly driven by European interest in using a local, renewable fuel. Modern wood pellet boilers have high efficiency and low pollutant emissions. Fiedler[7] reviewed the state of the art of small-scale pellet combustion units for domestic use and the individual European Union (EU) country regulations, where more stringent regulations are likely to appear in the future. Öhman et al.[8] studied the slagging tendencies in residential wood pellet boilers related to ash sintering temperatures. They found that wood pellets have a low sintering tendency (sintering temperatures higher than 1100 °C) mainly as a result of the low alkali and Si contents in the fuel.[9] Hence, modern wood pellet boilers use moving grates or sliding grate ash removal systems.[7] Better combustion chamber and flow geometry can be designed and optimized by applying computational fluid dynamics (CFD) simulations.[10,11] In addition, studies have shown that, when firing with non-woody biomass pellets, better boiler control, such as fuel feeding, air intake, and ash management, is required.[12]

A key index for assessing the performance of a wood pellet boiler is its thermal efficiency. There are many factors affecting the thermal efficiency of wood pellet boilers. Chandrasekaran et al. characterized the efficiency of two wood pellet boilers[13] and wood stoves burning multiple types of pellets.[14] Efficiencies ranged from 70 to 91% for different boilers running with wood pellets and from 75 to 85% when burning with non-woody pellets. Verma et al.[15,16] found that the performance of a domestic pellet boiler is a function of the boiler operational loads. Carlon et al.[17] reported a nonlinear relationship between thermal efficiency and a modified load factor. Several factors lead to the efficiency−load relationships. The most important factor is the excess air ratio that is usually higher under low-load conditions. In addition, low-load conditions cannot generate sufficient turbulence for complete combustion, which leads to low combustion efficiency and temperatures.[16] Heat transfer is also reduced during low-load conditions. Thus, it is better for the boiler to operate at high- or full-load conditions, so that maximum thermal efficiency can be achieved.
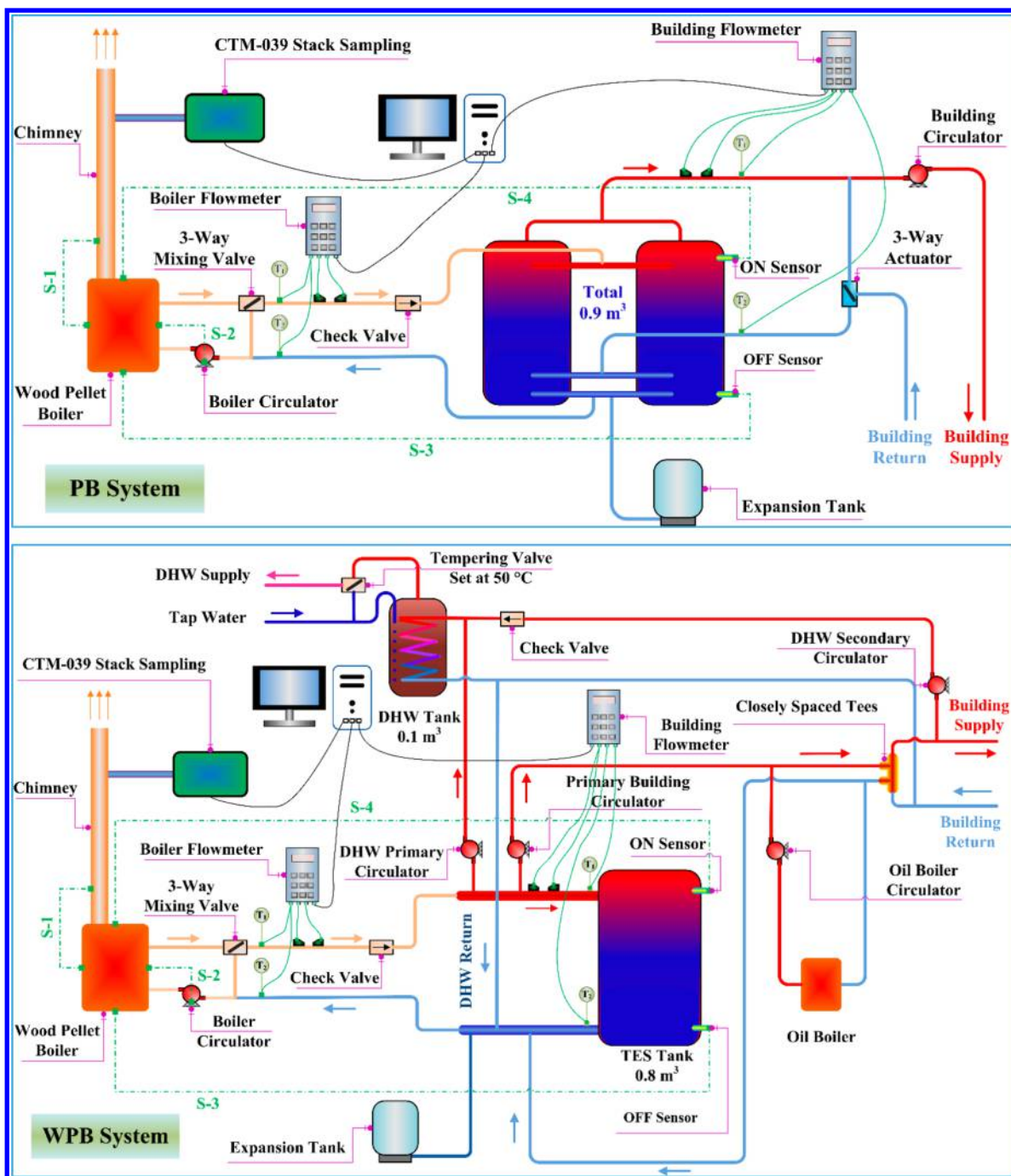
Figure 1. Schematic of the (top) PB and (bottom) WPB systems with data acquisition devices (S-1, flue gas O_2 control signal; S-2, boiler pump control signal; S-3, boiler on signal; and S-4, boiler off signal).

Dependent upon the building load and the ambient temperature, the building may not require all of the heat produced by the boiler when it operates at full load. The use of thermal energy storage (TES) enables the wood pellet boiler to operate for longer periods at higher loads and, consequently, reduces the number of boiler ignitions and avoids short cycling during warmer weather. TES in the form of large insulated water tanks was initially used in solar water heating systems because the stratification inside the tank can help to extract more useful heat from the tank.[18] Many experimental and numerical studies have been performed to study the performance of the TES tank in terms of temperature stratification, efficiency, and operational behavior.[19−25]

The present work systematically evaluated the performance of two modern wood pellet heating systems in terms of boiler thermal efficiency at various loads, TES tank discharge efficiency, and overall system efficiency based on long-term monitoring from 2015 to 2017. Currently, there are no such systematic evaluations of in-use wood pellet heating systems for such an extended period.

2. MATERIALS AND METHODS

2.1. Two Systems. In this project, two nominally identical 25 kW wood pellet boilers were installed in two homes in northern New York State with different configurations (as shown in Figure 1). In each boiler, wood pellets are fed by a stoker screw auger into the

combustion chamber from the top of the burner pot. A hot air gun ignites the pellets. Primary air enters the combustion chamber from the bottom of the burner pot. Hot combustion gas passes through a three-stage fire tube heat exchanger to transfer heat into jacket water and exhausts through the chimney. The induced draft fan at the end of the flue gas pathway controls the primary air flow through a lambda sensor (O_2 control, calibrated with an external combustion analyzer) and a negative pressure sensor (draft control). Within each fire tube, there is a twisted turbulator to improve heat transfer as well as to clean the inside surfaces of the fire tubes by moving the turbulators up and down. The residual ash is removed from the bottom ash collector. The boiler is controlled by software that records its operational data.

2.2. Pellet Fuel Characterization. The pellets used in this study are Pellet Fuels Institute (PFI[26])-certified premium pellets. Samples were collected during bulk delivery to the pellet bins. The pellets were characterized for heating value, moisture, composition, and ash content. Detailed analytical methods and results are listed in Table 1. The pellets have a mean calorific content of 19.12 MJ/kg (or 8221 Btu/lb) higher heating value (HHV), 3.88% moisture, 0.58% ash, and 46.64% carbon.

Table 1. Summary of Analytical Methods and Results

parameter	method	result
HHV (MJ/kg, ar)	ASTM E711-87 (2004)	19.12
moisture (%, wb)	ASTM E871-82 (2006)	3.88
ash (%, db)	ASTM D1102-84 (2007)	0.58
carbon (%, db)	ASTM E777-87 (2004)	46.64
hydrogen (%, db)	ASTM E777-87 (2004)	6.4
nitrogen (%, db)	ASTM E778-87 (1996)	0.14
oxygen (%, db)	by difference	46.23
chlorine (%, db)	ASTM E776-87 (2009)	0.00388
sulfur (%, db)	ASTM E775-87 (2004)	0.00689

2.3. Experimental Methods. Figure 1 shows the two system configurations as operated during the 2016−2017 heating season. These systems had each undergone modification over time, and detailed histories of each system are presented in the Supporting Information. The Parishville boiler (PB) system was installed in a modified shipping container near a family house in Parishville, NY, U.S.A. [44.63° N, 74.83° W, 271 m above sea level (a.s.l.)], replacing their existing outdoor wood boiler (OWB). Hot water from the boiler was stored in two identical TES tanks (A.O. Smith Co.; volume of each = 0.45 m³) and then delivered to the house for space heating through an underground circulation system. The tanks provided 36.0 L/kW (2.8 gallons kBtu⁻¹ h⁻¹) storage, above manufacturer recommendations of 25.7 L/kW (2 gallons kBtu⁻¹ h⁻¹). Return water from the building flowed to the bottom of the tanks. This house has a total heating area of 406.5 m², with an estimated peak load of 27 kW (92 000 Btu/h). The tanks store hot water from the boiler at temperature ranging from 55 °C (131 °F) to 75 °C (167 °F) that is used for a radiant floor heating system, with return water temperatures ranging from 35 °C (95 °F) to 45 °C (113 °F), depending upon the outdoor temperature and thermostat settings.

The other nominal 25 kW boiler was installed in the basement of a family house located in West Potsdam, NY, U.S.A. (44.69° N, 75.09° W, 122 m a.s.l.). An existing oil boiler was integrated into the system as an auxiliary boiler. This system is denoted as the West Potsdam boiler (WPB) system. A single 210 gallon TES tank (0.79 m³) was installed in the system. In this system, the TES tank was installed in a two-pipe configuration such that both the boiler and heat demand are on the same side of the tank. In addition, the WPB system had a 0.1 m³ domestic hot water (DHW) tank that provided domestic hot water. The additional oil boiler and DHW tank made both the system control and boiler behavior different from the PB system.

For both systems, flow and temperature were monitored in two loops, boiler to tank loop and tank to building loop, to calculate heat output from the boiler and TES tank, respectively. A certified

ultrasonic flow meter (EF-10 series, Spire Metering Technology) and two temperature probes were installed in each loop. The boiler was controlled by two temperature sensors in the TES tank (bottom on and top off).

To determine the energy input rate, the boiler stoker feed auger was calibrated at several feed rates. The pellets were collected in a weighed bucket, and after a fixed time, the bucket was weighed. From these results, the maximum feed rates (κ_{100}) were determined to be 12.98 and 12.17 kg/h for PB and WPB, respectively. The constant speed augers are modulated by operating them only part of the time (feed fraction, ε). The actual feed fractions are recorded at 1 s intervals by each boiler. Using the fuel characterization data, the heat input into the boiler can be calculated as the product of the mass flow rate and the calorific content of the pellets. It was found that the augers were quite reproducible over time such that multiple calibrations produced essentially identical relationships between the time of auger operation and mass flow rates of fuel delivered into the boiler.

The operation of these boiler−thermal storage systems was characterized in terms of "system cycles" that began with the startup of the boiler, steady-state combustion, boiler shutdown, and finally depletion of heat from the thermal storage system to the building until the boiler restarted because the control temperature at the top of the thermal storage tank had been reduced to the set point value. Within these system cycles, there are "boiler cycles". A complete boiler cycle includes three phases: startup, steady-state combustion, and burnout/shutdown.

For the PB system, measurements were made over three heating seasons denoted as PB-1, PB-2, and PB-3. PB-1 included data from February 1, 2015 to April 11, 2015, representing 493 cycles; PB-2 included data from December 1, 2015 to April 1, 2016, with a total of 392 cycles; and PB-3 included data from January 5, 2017 to April 5, 2017, with a total of 372 cycles. During PB-1 and PB-2, the thermal storage tanks were continuously connected to the circulation loop that conducted heat to the building (see Figure SI-3 of the Supporting Information). Water was continuously circulated through this loop to avoid freezing in the underground line. Before PB-3, a three-way valve was installed (top of Figure 1) such that the circulation loop was separated from the thermal storage tanks when there was no demand for heat from the house. Local weather data obtained from Weather Underground[27] were used in this study.

For the WPB system, major changes had been made over the prior heating seasons to address operational problems that had been identified (see the Supporting Information). Thus, only WPB-3 data were used for the performance analysis. WPB-3 ran from December 28, 2016 to April 12, 2017 and included a total of 644 cycles.

2.4. Efficiency Calculations. Because of the slower startup and shutdown associated with solid fuel combustion, the boiler thermal efficiency was calculated on the basis of each boiler cycle. Overall efficiency was calculated on the basis of system cycles. For each boiler cycle, the boiler thermal efficiency (η_{th}) was calculated as the ratio of heat output/heat input over each cycle time (t_c)

$$\eta_{th} = \frac{\sum_0^{t_c} [Q\rho_w c_{p,w}(T_1 - T_2)\Delta t_i]}{\sum_0^{t_c} (HHV\kappa_{100}\varepsilon_i)} \times 100\% \tag{1}$$

where Δt is the ultrasonic flowmeter data sampling interval (10 s). The boiler stoker feed fraction ε was recorded every 1 s.

System efficiency is defined on the basis of system cycles. It is the total energy delivered into the building during a system cycle divided by the total energy input into the boiler for each boiler cycle as

$$\eta_{sys} = \frac{\sum_0^{t_c+t_d} [Q^*\rho_w c_{p,w}(T_1^* - T_2^*)\Delta t_i]}{\sum_0^{t_c} (HHV\kappa_{100}\varepsilon_i)} \times 100\% \tag{2}$$

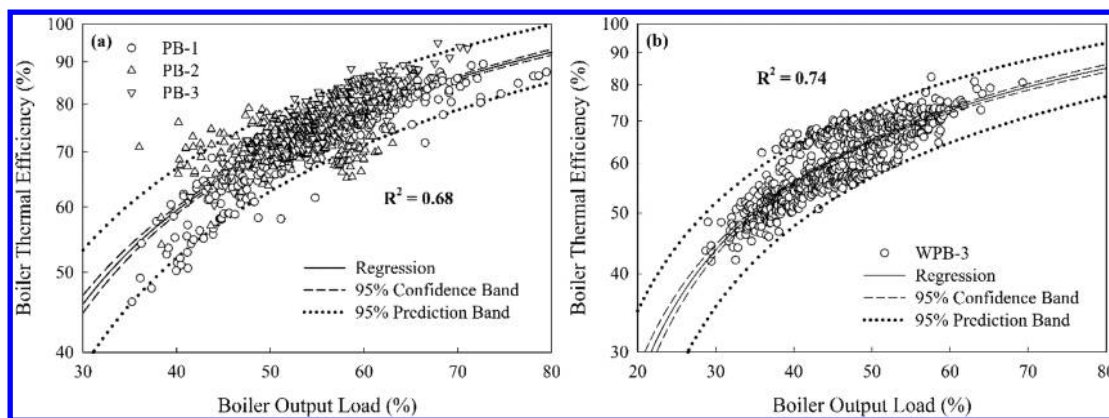where t_d is the time when the boiler is off until the next boiler cycle.

Figure 2. Correlations between boiler thermal efficiency and boiler output load for the (a) PB and (b) WPB boiler systems.
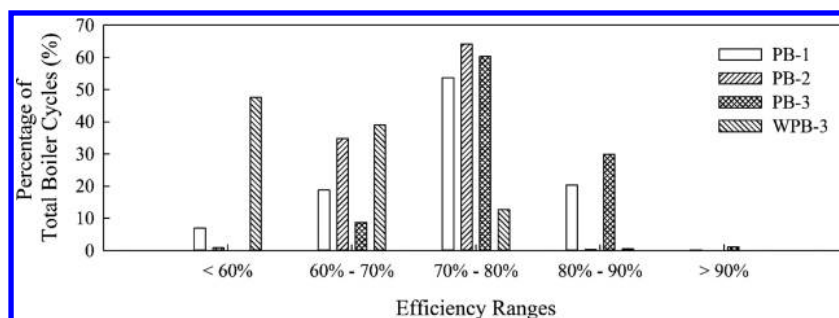

Figure 3. Boiler thermal efficiency bins for the PB and WPB systems.

3. RESULTS AND DISCUSSION

3.1. Boiler Thermal Efficiency. During a boiler cycle, the instantaneous efficiency of the boiler changes. Low efficiency occurs during startup as a result of inefficient combustion during the ignition and stabilization stages when there are also high CO and particle emissions.[28] As the combustion stabilizes, the boiler thermal efficiency reaches its highest value during its steady-state operation. Low efficiencies again occur as the boiler shuts down and the residual fuel burns out. Thus, boiler thermal efficiency over each cycle is an appropriate metric for boiler performance.

Figure 2 shows the regression between boiler thermal efficiency and boiler output load percentage for both boiler systems. For the PB system, as a result of boiler software updates and frequent setting change of TES tank on/off temperatures during PB-2 and PB-3, a relatively low $r^2 = 0.68$ was determined. However, when these parameters remained fixed in PB-1, r^2 rose to 0.86. For the WPB system, the operation of DHW significantly affected the boiler cycling characteristics, as explained in the Supporting Information. Because the DHW tank represented a low thermal mass, very little energy was dissipated into the domestic hot water. When the boiler was on because of the demand from the thermal storage tank and the DHW was also demanding heat, the DHW tank acts as an independent TES tank. However, the low heat dissipation in the DHW tank resulted in very high boiler return water temperatures that approached the safety limit set temperature of the boiler. Therefore, the boiler reduced its output quickly, sometimes causing boiler short cycling. The problem was reduced during WPB-3 by defining wider temperature set points for the DHW tank, but controls alone could not eliminate the problem.

A general regression equation based on four data sets for the two systems was determined by merging the data and fitting an equation as follows:

$$\eta_{th} = 52.69 \ln \chi - 137.7 \qquad \text{(for } 25 < \chi < 75\text{)} \qquad (3)$$

There was a moderately good fit with $r^2 = 0.79$. Boiler output load percentage χ is calculated as the ratio of boiler actual output to the nominal output during a cycle, as shown in eq 4

$$\chi = \frac{\sum_0^{t_c}[Q\rho_w c_{p,w}(T_1 - T_2)\Delta t]}{3600 N t_c} \times 100\% \qquad (4)$$

where N is the boiler nominal output capacity.

The regression in eq 3 is comparable to the results of Carlon et al.,[17] where they related thermal efficiency to a modified output load factor using boiler combustion time. Equation 3 provides a direct relationship for the boiler output load percentage without any modifications. Equation 3 also indicates that, for best performance, it is necessary to operate the boiler within its highest output range. Hence, the TES tank can increase system efficiency by storing the extra energy from the boiler when the heat demand from the building decreases. Equation 3 also suggests that modulation for wood pellet boilers may not be a good choice if the modulation is at the expense of boiler efficiency.

Equation 3 can be interpreted by dividing eq 1 by eq 4 to produce eq 5.

$$\frac{\eta_{th}}{\chi} = \frac{3600N}{HHV\kappa_{100}\varepsilon_i} \qquad (5)$$

Therefore, the change of boiler feed fraction ε produces a change in the ratio of efficiency and load, resulting in the
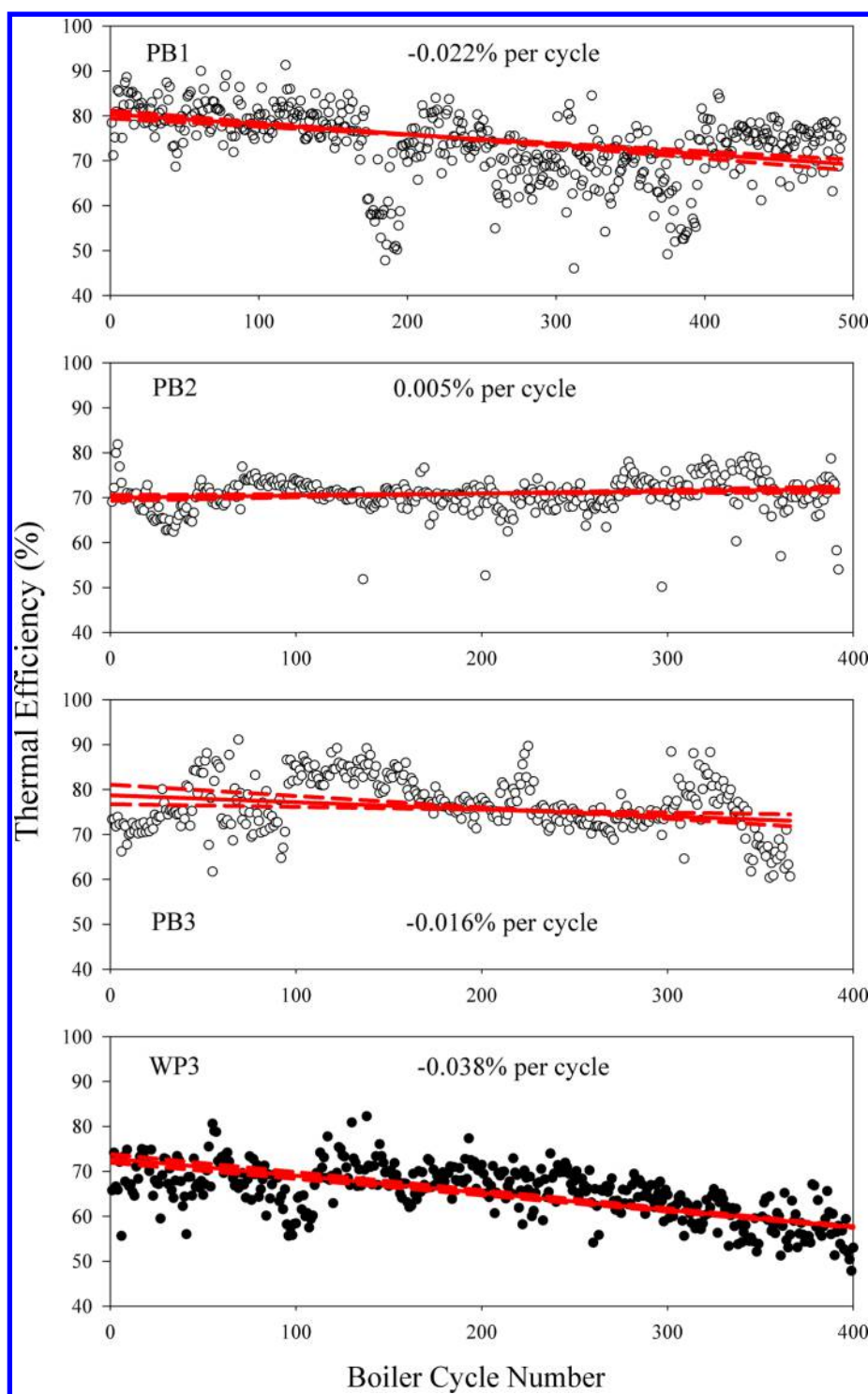
Figure 4. Sen's slope of boiler thermal efficiency for the PB and WPB system (c.i. = confidence interval) process. Thus, operation of a dehumidifier in these circumstances may improve the boiler performance.

logarithmic relationship between the two parameters shown in Figure 2.

   The relatively widespread data shown in Figure 2 could be caused by several reasons. For PB, a wide range of boiler on/off temperature settings were tried from 40 to 75 °C during PB-2 and PB-3. Therefore, PB-1 had relatively narrower spread than PB-2 and PB-3 because a constant boiler on/off temperature setting was used. In addition, several boiler software updates were performed during PB-2 and PB-3, which further increases

the data spread. For WPB, the wide range of data spread was mainly due to frequent short cycling of the boiler, which will be discussed in the Supporting Information.

   Figure 3 shows the binned boiler thermal efficiencies during the monitored period for both systems. Over 50% of boiler cycles operated above 70% thermal efficiency for PB-1 (74.3% of total), PB-2 (64.4% of total), and PB-3 (91.3% of total). The percentage of boiler cycles with efficiency above 80% for PB-1, PB-2, and PB-3 was 20.6, 0.3, and 31.0%, respectively. The lack

of high-efficiency boiler cycles for PB-2 resulted from the lack of manual cleaning of the system from PB-1 to PB-2 and relying only on the internal cleaning mechanism of the boiler. After two manual cleanings performed during PB-3, the overall boiler thermal efficiency for PB-3 improved significantly. The overall seasonal average boiler thermal efficiency for PB-1, PB-2, and PB-3 was 73.6, 70.8, and 79.0%, respectively. Those seasonal average efficiency values are comparable to most of the reported field test boiler efficiency values from similar wood pellet boiler studies.[14−16,29]

In comparison to PB, WPB had much lower boiler thermal efficiencies, with 87% of WPB-3 boiler cycles operating below 70% thermal efficiency and only 13% of WPB-3 boiler cycles above 70% thermal efficiency. This poorer performance was caused by the generally lower loads for the WPB system compared to the PB system, as indicated in Figure 2. As mentioned in the Supporting Information, the load reduction was caused by the two-pipe system design that incorporated the low thermal mass DHW tank and the resulting high boiler return water temperatures. A possible solution would be to switch the DHW return water from the location shown in Figure 1 to an intermediate location on the right side of the TES tank, resulting in a three-pipe configuration. However, there was no opportunity to try this approach within this project.

Figure 3 also shows that there was a small fraction of cycles when the boiler operated at efficiencies greater than 90% during PB-3. These high efficiencies were observed during the longer cycle times. The average cycle times were 1.4, 2.5, and 2.2 h for PB-1, PB-2, and PB-3 periods, respectively. Increases in boiler cycle length will decrease the fraction of low efficiency stages (ignition, stabilization, and burnout stages) and, thus, generally increase the overall cycle efficiency. A wide on/off temperature range and/or high building heat demand will increase the boiler cycle times significantly.

3.2. Trend Analysis on Boiler Thermal Efficiency. By examination of the thermal efficiency for each boiler cycle, the rate at which the boiler efficiency decreases can be determined. Because the data are not normally distributed, a Mann−Kendall (MK) analysis with Sen's slope[30,31] was performed. The hypothesis is that the analyzed data have a monotonic trend. The MK test is based on the test statistic S defined as

$$S = \sum_{i=1}^{n-1} \sum_{j=i+1}^{n} \text{sgn}(x_j - x_i)$$

(6)

where x_j and x_i are data values ($j > i$), n is the number of total data points, and $\text{sgn}(x_j - x_i)$ is the sign function defined as

$$\text{sgn}(x_j - x_i) = \begin{cases} +1, & x_j - x_i > 0 \\ 0, & x_j - x_i = 0 \\ -1, & x_j - x_i < 0 \end{cases}$$

(7)

Mann[30] and Kendall[31] have shown that, when $n \geq 18$, S is approximately a normal distribution with expectation of 0 and variance as

$$\sigma^2(S) = \frac{n(n-1)(2n+5) - \sum_{i=1}^{m} t_i(t_i - 1)(2t_i + 5)}{18}$$

(8)

where m is the number of tied groups and t_i denotes the number of ties of extent i. A tied group is defined as a set of samples with the same value. The standard normal test (or Z test) statistic Z_S is computed as

$$Z_S = \begin{cases} \dfrac{S - 1}{\sqrt{\sigma^2(S)}}, & \text{if } S > 0 \\ 0, & \text{if } S = 0 \\ \dfrac{S + 1}{\sqrt{\sigma^2(S)}}, & \text{if } S < 0 \end{cases}$$

(9)

$Z_S > 0$ means increasing trends, while $Z_S < 0$ means decreasing trends. A Theil−Sen line is usually used to estimate the slope of the trend (also called Sen's slope analysis). Figure 4 shows the analysis results for PB and WPB systems.

A decreasing trend in boiler thermal efficiency can be observed in Figure 4a when there was no manual cleaning performed. High boiler thermal efficiency of around 85% was initially observed after the boiler installation. An average rate of −0.022% per boiler cycle was determined for PB-1. Therefore, if the boiler must be cleaned manually when the thermal efficiency has dropped by 10%, PB has to be cleaned after 455 boiler cycles. Given an average of 7 boiler cycles per day, the boiler needs to be cleaned after ∼65 days of continuous operation. Figure 4b shows a relatively constant trend of boiler thermal efficiency for PB-2, which suggests that the boiler can only maintain around 70% thermal efficiency based on its internal cleaning mechanism. After two manual cleanings were performed during PB-3, the boiler thermal efficiency significantly improved in comparison to PB-2. For WPB-3, an average boiler thermal efficiency rate of −0.038% per boiler cycle was determined, which means WPB must be manually cleaned after 263 boiler cycles or ∼38 days of continuous operation given the same evaluating criterion as PB. WPB-3 had the higher rate of decline in the boiler thermal efficiency. One factor for this boiler could be the high moisture content in the basement. This old basement has little ventilation, and standing water was often observed on the basement floor on rainy days. When the boiler was manually cleaned at the beginning of WPB-3, the cleaning turbulators had to be replaced as a result of substantial fouling and corrosion. In a high-moisture environment, it is much easier to have condensation in the boiler, which facilitates boiler fouling and corrosion.

3.3. Thermal Storage Tank Performance. The TES tank top and bottom temperatures are measured by the on and off temperature sensors inserted into sensor wells in the tank, as shown in Figure 1. The TES tank top and bottom temperature difference (ΔT_s) can be used to assess tank stratification because a well-stratified tank has a larger ΔT_s. Figure 5 shows tank behavior during a complete system cycle in PB-1.

The vertical dashed lines divide the system cycle into charge and discharge periods. During the TES tank charging period, the boiler heats the tank to the set temperature. Then, the boiler shuts down, and the tank discharges heat to the building. The amount of energy discharged is determined by the stratification inside the tank because a well-stratified tank has higher exergy than a completely mixed tank.[32] The TES tank can continuously supply energy to the building without interruption depending upon the building demand.
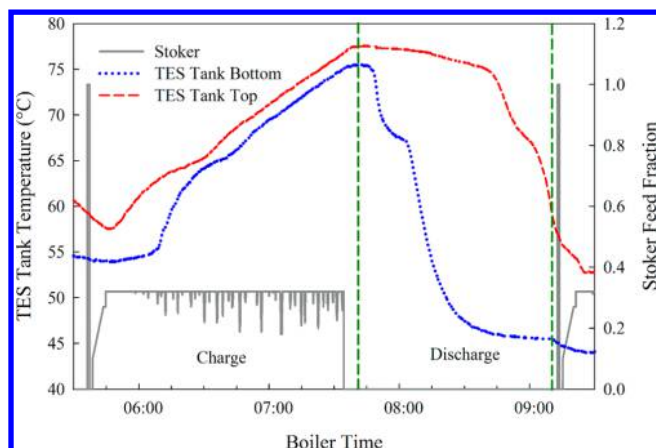
Figure 5. TES tank temperature distribution during one complete boiler burn cycle in PB-3.

A well-stratified tank can discharge more energy than a completely mixed tank, as shown in earlier studies.[19−24] The overall tank efficiency (φ) is defined as

$$\varphi = (E_{cha} + E_{dis})/B_{total} \times 100\% \tag{10}$$

Simultaneously, tank discharge efficiency (φ_{dis}) is defined as

$$\varphi_{dis} = E_{dis}/(B_{total} - E_{cha}) \times 100\% \tag{11}$$

where E_{cha} and E_{dis} are energy delivered to the building during charge and discharge periods, respectively, and B_{total} is the total energy delivered to the tank during a complete boiler cycle.

Tank discharge efficiency, φ_{dis}, is a good indicator of the stratification inside the tank when the boiler is off. Studies have shown that two major factors affect the stratification: tank geometry (inlet/outlet positions,[20] tank aspect ratio,[19] baffle plates,[23] etc.) and operational conditions (temperature difference,[33] flow rates,[33] operation modes,[21,22] etc.). The present evaluation focuses on these operational conditions because the tanks had a fixed geometry during the entire monitoring period and the TES tank was operated with continuous flow on the building side for the PB system during the first two heating seasons.

Figure 6a shows TES tank top and bottom average temperature difference ($\Delta T_{s,ave}$) over each discharge period as a function of the corresponding discharge time t_d (or boiler off time) for PB-1 data. The correlation equation is shown below ($r^2 = 0.83$).

$$\Delta T_{s,ave} = 66.75(t_d)^{-1} - 150.0(t_d)^{-2} + 119.3(t_d)^{-3} - 5.965 \tag{12}$$

Longer discharge times indicate less heat demand from the building (i.e., warmer weather) that result in smaller temperature differences in the tank because the TES tank supply and return water temperatures will be closer in temperature. Then, no clear thermocline may develop in the tank.[34] Consequently, when the building is demanding heat, a larger $\Delta T_{s,ave}$ will occur as a result of the larger temperature difference between the TES tank supply and return water temperatures. Figure 6a shows that stratification of a TES tank in the heating system is highly dependent upon the building heat load. This result suggests that maintaining stratification inside the tank at low building heat loads can be attained by decreasing the flow rate to create a larger return water temperature difference from the tank top temperature.

Figure 6b shows TES tank discharge efficiency φ_{dis} correlated with a dimensionless number ξ by the following equation ($r^2 = 0.73$):

$$\ln \varphi_{dis} = 8.3 - 175.3\xi \tag{13}$$

where φ_{dis} is in percent and ξ is expressed in pipe Reynolds number (Re_d) and temperature differences as

$$\xi = (\Delta T_{s,ave}/\Delta T_{d,ave})^{0.35}(Re_d)^{-0.41} \tag{14}$$

where $\Delta T_{s,ave}$ is the average TES tank top and bottom temperature difference during discharge period and $\Delta T_{d,ave}$ is the average TES tank supply and return temperature difference during the same discharge period. Figure 6b indicates that an increase in Re_d and decrease in $\Delta T_{s,ave}/\Delta T_{d,ave}$ will lead to an exponential increase in tank discharge efficiency. For a specific TES tank, increasing Re_d means an increased flow rate, which corresponds with previous studies that the TES tank discharge efficiency (or extraction efficiency) increases with an increasing flow rate.[19,24,33] Thus, inlet flow diffusers and baffles[23,24,35] are used to minimize flow mixing and maintain a high level of stratification. The ratio of $\Delta T_{s,ave}/\Delta T_{d,ave}$ is an indicator of the amount of heat delivered to the building. The maximum value of $\Delta T_{s,ave}/\Delta T_{d,ave}$ is 1 when there is no heat delivered to the building or the return water temperature is equal to the temperature at the bottom of the TES tank. Small ratios suggest large TES tank supply and return temperature differences, which further indicate large amounts of heat consumed by the building.

For PB-2 and PB-3, correlations between $\Delta T_{s,ave}$ and t_d, φ_{dis}, and ξ have much lower r^2 values compared to PB-1 data. This
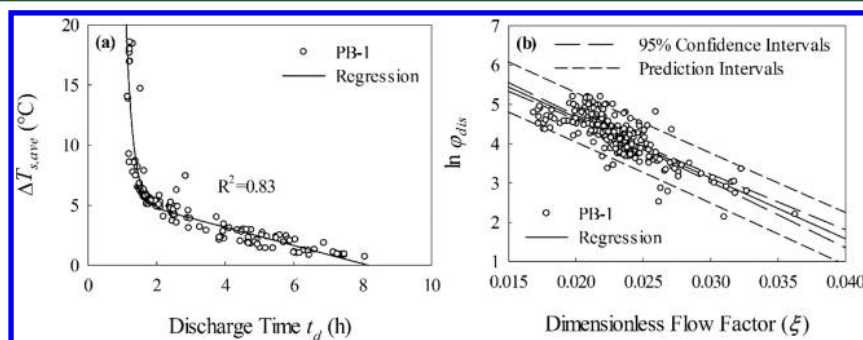

Figure 6. (a) TES tank top and bottom average temperature difference as a function of the discharge time for PB-1 and (b) tank discharge efficiency correlated with the dimensionless flow factor for PB-1.

result is caused by the constant TES tank on/off setting maintained over the whole heating season for PB-1, but a variety of TES tank on/off settings were explored during PB-2 and PB-3 that, in turn, reduced the correlation. For WPB-3, the TES tank stratification (ΔT_s) was constantly disturbed by the DHW tank operation. Therefore, the correlation was worse than for PB-2 and PB-3. In addition, the two-pipe configuration prohibits the determination of the exact amount of energy delivered into the TES tank because part of the energy produced while the boiler is on can be directed to the DHW tank. Therefore, no correlation for TES tank discharge efficiency can be established. An additional flowmeter on the DHW tank loop would have been required to permit this calculation.

3.4. System Efficiency. System efficiency evaluates the efficiency of the whole system based on the heat delivered to the building and the heat input into the boiler. The average seasonal system efficiency values were 62.8, 62.0, and 75.8% for PB-1, PB-2, and PB-3, respectively. Low system efficiencies during PB-1 and PB-2 was mostly due to the low thermal efficiencies and low TES tank discharge efficiencies when there was no three-way valve installed to prevent the constant circulation of the building circulator, as shown in Figure 1 (as discussed in the Supporting Information). After effective boiler cleaning and system modification, the system efficiency in PB-3 significantly increased. System efficiencies for WPB could not be calculated because the current measurement system did not permit the determination of the amounts of heat input transferred into both the TES tank and the building based on the two-pipe configuration system.

4. CONCLUSIONS AND SUGGESTIONS

4.1. Conclusions. The objective of this study was to evaluate the performance of two 25 kW residential wood pellet boilers in terms of boiler thermal efficiency, TES tank discharge efficiency, and system efficiency based on long-term field site monitoring results. A general correlation between boiler thermal efficiency (η_{th}, %) and boiler output load percentage (χ, %) was determined to be $\eta_{\text{th}} = 52.69 \ln \chi - 137.7$, with $r^2 = 0.79$ (for $25 < \chi < 75$), for both systems. Evaluation of thermal efficiency bins showed that, most of the time, the PB boiler was operating above 70% efficiency with seasonal average thermal efficiencies of 73.6, 70.8, and 79.0% for PB-1, PB-2, and PB-3, respectively. However, the WPB boiler was operating below 70% thermal efficiency most of the time caused by the DHW-induced load modulation and severe boiler fouling. Sen's slope analysis on the boiler thermal efficiency can determine the boiler thermal efficiency decreasing rate and provide information on when additional cleaning is needed. The results showed that the PB boiler had a thermal efficiency drop of 0.022% per boiler cycle and could maintain around 70% boiler thermal efficiency without manual cleaning. The WPB boiler had a thermal efficiency drop of 0.038% per boiler cycle and must be cleaned every 38 days (given an average of 7 boiler cycles per day). TES tank performance showed a correlation of the tank discharge efficiency with a dimensionless number that is a function of inlet pipe Reynolds number and temperature differences in both the tank and pipe inlet/outlet. The system efficiency evaluation revealed that effective boiler cleaning and system modification can enhance overall system performance. Overall system efficiency showed seasonal averages of 62.8, 62.0, and 75.8% for PB-1, PB-2, and PB-3, respectively. Future work will be focused on continuing to monitor and perform

dynamic process simulation of the system for further optimization. The boiler emissions will be discussed separately in a future paper.

4.2. Suggestions for Improvement. (1) High moisture content in the combustion air can accelerate wood pellet boiler fouling, as shown in WPB installation. Therefore, it is important to ensure a low-moisture-content environment for the wood pellet boiler, such as adding a dehumidifier to a high-moisture-content environment. (2) The two-pipe configuration does not necessarily perform better than the traditional four-pipe configuration. It is important to recognize the effect of the thermal mass of the different heat-demanding units connected to the system such that the boiler short cycling and load modulation shown in the WPB system can be avoided. An alternative three-pipe configuration might solve the problem. (3) Frequent manual cleaning of the heat exchanger is essential to maintaining high overall system performance for these wood pellet heating systems. The decline in the thermal efficiency can serve as an indicator of the need for additional cleaning.

■ ASSOCIATED CONTENT

ⓢ Supporting Information

The Supporting Information is available free of charge on the ACS Publications website at DOI: 10.1021/acs.energy-fuels.7b01868.

Introduction on PB and WPB wood pellet boiler heating systems (PDF)

■ AUTHOR INFORMATION

Corresponding Author
*E-mail: phopke@clarkson.edu.

ORCID ⓞ
Kui Wang: 0000-0003-4743-5442
Philip K. Hopke: 0000-0003-2367-9661

Notes
The authors declare no competing financial interest.

■ ACKNOWLEDGMENTS

■ NOMENCLATURE

B_{total} = energy to the tank from boiler (kJ)
$c_{\text{p,w}}$ = water specific heat (kJ kg^{-1} K^{-1})
E_{cha} = energy to building during tank charge (kJ)
E_{dis} = energy to building during tank discharge (kJ)
HHV = pellet fuel higher heating value (MJ/kg)
M_{w} = pellet fuel moisture content (%, wb)
N = boiler nominal load (kW)
Q = boiler loop flow rate (m^3/h)
Q^* = building loop flow rate (m^3/h)
Re_{d} = inlet pipe Reynolds number

t_c = time of a complete burn cycle (h)

t_d = boiler off time or tank discharge time (h)

T_1 = boiler output water temperature (°C)

T_1^* = TES tank output water temperature (°C)

T_2 = boiler return water temperature (°C)

T_2^* = TES tank return water temperature (°C)

Δt = boiler flow meter recording interval (s)

ΔT_d = TES tank inlet/outlet temperature difference (°C)

$\Delta T_{d,ave}$ = average TES tank inlet/outlet temperature difference during discharge (°C)

ΔT_s = TES tank top and bottom temperature difference (°C)

$\Delta T_{s,ave}$ = average TES tank top and bottom temperature difference during discharge (°C)

ε = boiler stoker feed fraction

η_{th} = boiler thermal efficiency (%)

η_{sys} = system efficiency (%)

κ_{100} = boiler stoker feed rate at 100% (kg/h)

ξ = TES tank flow factor

ρ_w = water density (kg/m^3)

φ = TES tank overall efficiency (cycle basis, %)

φ_{dis} = TES tank discharge efficiency (%)

χ = boiler output load (%)

■ REFERENCES

(1) International Energy Agency (IEA). *Our Work on Renewables*; IEA: Paris, France, 2017; https://www.iea.org/topics/renewables/subtopics/bioenergy/.

(2) International Energy Agency (IEA). *Biofuels Can Provide up to 27% of World Transportation Fuel by 2050, IEA Report Says—IEA 'Roadmap' Shows How Biofuel Production Can Be Expanded in a Sustainable Way, and Identifies Needed Technologies and Policy Actions*; IEA: Paris, France, 2011; https://www.iea.org/newsroomandevents/pressreleases/2011/april/biofuels-can-provide-up-to-27-of-world-transportation-fuel-by-2050-iea-report-.html.

(3) Demirbas, A. Biomass resource facilities and biomass conversion processing for fuels and chemicals. *Energy Convers. Manage.* **2001**, *42*, 1357−1378.

(4) Goh, C. S.; Junginger, M.; Cocchi, M.; Marchal, D.; Thrän, D.; Hennig, C.; Heinimö, J.; Nikolaisen, L.; Schouwenberg, P.-P.; Bradley, D.; Hess, R.; Jacobson, J.; Ovard, L.; Deutmeyer, M. Wood pellet market and trade: A global perspective. *Biofuels, Bioprod. Biorefin.* **2013**, *7*, 24−42.

(5) Parikka, M. Global biomass fuel resources. *Biomass Bioenergy* **2004**, *27*, 613−620.

(6) Chau, J.; Sowlati, T.; Sokhansanj, S.; Preto, F.; Melin, S.; Bi, X. Techno-economic analysis of wood biomass boilers for the greenhouse industry. *Appl. Energy* **2009**, *86*, 364−371.

(7) Fiedler, F. The state of the art of small-scale pellet-based heating systems and relevant regulations in Sweden, Austria and Germany. *Renewable Sustainable Energy Rev.* **2004**, *8*, 201−221.

(8) Öhman, M.; Boman, C.; Hedman, H.; Nordin, A.; Boström, D. Slagging tendencies of wood pellet ash during combustion in residential pellet burners. *Biomass Bioenergy* **2004**, *27*, 585−596.

(9) Vega-Nieva, D. J.; Ortiz Torres, L.; Míguez Tabares, J. L.; Morán, J. Measuring and Predicting the Slagging of Woody and Herbaceous Mediterranean Biomass Fuels on a Domestic Pellet Boiler. *Energy Fuels* **2016**, *30*, 1085−1095.

(10) Porteiro, J.; Collazo, J.; Patiño, D.; Granada, E.; Moran Gonzalez, J. C.; Míguez, J. L. Numerical modeling of a biomass pellet domestic boiler. *Energy Fuels* **2009**, *23*, 1067−1075.

(11) Chaney, J.; Liu, H.; Li, J. An overview of CFD modelling of small-scale fixed-bed biomass pellet boilers with preliminary results from a simplified approach. *Energy Convers. Manage.* **2012**, *63*, 149−156.

(12) Carvalho, L.; Wopienka, E.; Pointner, C.; Lundgren, J.; Verma, V. K.; Haslinger, W.; Schmidl, C. Performance of a pellet boiler fired with agricultural fuels. *Appl. Energy* **2013**, *104*, 286−296.

(13) Chandrasekaran, S. R.; Laing, J. R.; Holsen, T. M.; Raja, S.; Hopke, P. K. Emission characterization and efficiency measurements of high-efficiency wood boilers. *Energy Fuels* **2011**, *25*, 5015−5021.

(14) Chandrasekaran, S. R.; Hopke, P. K.; Newtown, M.; Hurlbut, A. Residential-scale biomass boiler emissions and efficiency characterization for several fuels. *Energy Fuels* **2013**, *27*, 4840−4849.

(15) Verma, V. K.; Bram, S.; Gauthier, G.; De Ruyck, J. Performance of a domestic pellet boiler as a function of operational loads: Part-2. *Biomass Bioenergy* **2011**, *35*, 272−279.

(16) Verma, V. K.; Bram, S.; Delattin, F.; De Ruyck, J. Real life performance of domestic pellet boiler technologies as a function of operational loads: A case study of Belgium. *Appl. Energy* **2013**, *101*, 357−362.

(17) Carlon, E.; Schwarz, M.; Golicza, L.; Verma, V. K.; Prada, A.; Baratieri, M.; Haslinger, W.; Schmidl, C. Efficiency and operational behaviour of small-scale pellet boilers installed in residential buildings. *Appl. Energy* **2015**, *155*, 854−865.

(18) Hollands, K. G. T.; Lightstone, M. F. A review of low-flow, stratified-tank solar water heating systems. *Sol. Energy* **1989**, *43*, 97−105.

(19) Lavan, Z.; Thompson, J. Experimental study of thermally stratified hot water storage tanks. *Sol. Energy* **1977**, *19*, 519−524.

(20) Shah, L. J.; Furbo, S. Entrance effects in solar storage tanks. *Sol. Energy* **2003**, *75*, 337−348.

(21) Fernandez-Seara, J.; Uhia, F. J.; Sieres, J. Experimental analysis of a domestic electric hot water storage tank. Part I: Static mode of operation. *Appl. Therm. Eng.* **2007**, *27*, 129−136.

(22) Fernandez-Seara, J.; Uhia, F. J.; Sieres, J. Experimental analysis of a domestic electric hot water storage tank. Part II: Dynamic mode of operation. *Appl. Therm. Eng.* **2007**, *27*, 137−144.

(23) Ievers, S.; Lin, W. Numerical simulation of three-dimensional flow dynamics in a hot water storage tank. *Appl. Energy* **2009**, *86*, 2604−2614.

(24) Han, Y. M.; Wang, R. Z.; Dai, Y. J. Thermal stratification within the water tank. *Renewable Sustainable Energy Rev.* **2009**, *13*, 1014−1026.

(25) Rosen, M. A.; Dincer, I. Exergy methods for assessing and comparing thermal storage systems. *Int. J. Energy Res.* **2003**, *27*, 415−430.

(26) Pellet Fuels Institute (PFI). *Joining the PFI Standards Program*; PFI: Seattle, WA, 2017; http://www.pelletheat.org/joining-the-standards-program.

(27) Weather Underground. *Weather History & Data Archive*; Weather Underground: San Francisco, CA, 2017; https://www.wunderground.com.

(28) Win, K.; Persson, T. Emissions from residential wood pellet boilers and stove characterized into start-up, steady operation, and stop emissions. *Energy Fuels* **2014**, *28*, 2496−2505.

(29) Sippula, O.; Hytönen, K.; Tissari, J.; Raunemaa, T.; Jokiniemi, J. Effect of wood fuel on the emissions from a top-feed pellet stove. *Energy Fuels* **2007**, *21*, 1151−1160.

(30) Mann, H. B. Nonparametric tests against trend. *Econometrica* **1945**, *13*, 245−259.

(31) Kendall, M. G. *Rank Correlation Methods*; Griffin: London, U.K., 1975.

(32) Rosen, M. A. The exergy of stratified thermal energy storages. *Sol. Energy* **2001**, *71*, 173−185.

(33) Hariharan, K.; Badrinarayana, K.; Srinivasa Murthy, S.; Krishna Murthy, M. V. Temperature stratification in hot-water storage tanks. *Energy* **1991**, *16*, 977−982.

(34) Abdoly, M. A.; Rapp, D. Theoretical and experimental studies of stratified thermocline storage of hot water. *Energy Convers. Manage.* **1982**, *22*, 275−285.

(35) Altuntop, N.; Arslan, M.; Ozceyhan, V.; Kanoglu, M. Effect of obstacles on thermal stratification in hot water storage tanks. *Appl. Therm. Eng.* **2005**, *25*, 2285−2298.